2012

Fault and fracture zone detection based on soil gas mapping and gamma ray survey at the extension site of an open pit coal mine

Ya Ma
University of Queensland

Detlef Bringemeier
Golder Associates, Toowong

Alexander Scheuermann

Tiro Molebatsi

Ling Li

FAULT AND FRACTURE ZONE DETECTION BASED ON SOIL GAS MAPPING AND GAMMA RAY SURVEY AT THE EXTENSION SITE OF AN OPEN PIT COAL MINE

Ye Ma[1], Detlef Bringemeier[2], Alexander Scheuermann, Tiro Molebatsi and Ling Li

ABSRACT: Identification of open active faults and fracture zones is a part of exploration study prior to mining operation. However, detailed mapping of geological discontinuities in an otherwise low permeable overburden is rarely carried out in the mining area. To develop a rapid and feasible survey method, a field campaign was conducted to examine different soil gas survey methods along three transects at the Carrington West Wing extension site of a coal mine, Hunter River Valley, NSW, Australia. Coal seam gas together with Uranium-238 (present in the gas-bearing coal seam) increases the soil gas signal which can be detected with suitable soil gas mapping methods. Three techniques associated with four parameters were tested at the field site. A conventional active soil gas sampling method was applied with the samples analysed off-site in the lab by gas chromatography for carbon dioxide and methane concentrations. Radon was measured on site by means of radon detector. It was expected that high soil gas concentration anomalies, if detected, could then be related to the locations of permeable fault/ fracture zones. A rapid and simple technique was used to determine the relative counts of Bismuth-214 in the soil surface by employing a gamma ray spectrometer. As a decay product of the ^{222}Rn, ^{214}Bi is also expected to exhibit relatively higher activities in the soil over faults and fracture zones.

INTRODUCTION

Open-cut is a commonly applied mining method in the Hunter River Valley and other Australian coal mining regions. By removing the overburden above the coal seam, this surface mining operation creates a significant drainage potential for the surrounding environment, like the adjacent river and the groundwater systems. The NSW Office of Water proposed a new NSW aquifer interference policy to protect the groundwater system, because of the significant growth of the coal and coal seam gas industries (The NSW Office of Water, 2011). Most previous studies focussed on the shallow aquifer investigation, without further study of the fracture flow in the rock overburden in the Hunter River Valley (Mackie, 2010). However, the mining impacts on the adjacent river and groundwater systems are likely to be controlled predominately by preferential flow zones provided by faults, fracture and coal seam cleats (López and Smith, 1995). Therefore, how to characterise hydraulic connectivity of faults/fractures with a river and alluvial aquifers and how to locate these permeable structures are becoming very critical questions for the groundwater risk assessment and mine water management. In this context, the non-invasive soil gas mapping method and gamma ray spectrometer reconnaissance are discussed and examined for the purpose of detecting the location of structures.

Soil gas mapping is based on measurements of the gases contained in the interstitial spaces of the soil above the water table and capillary fringe. Soil gases, including methane, carbon dioxide and radon, are sampled and analysed. Thermal methane is formed as part of the process of coal formation - coalification. It is released as a result of natural erosion or faulting. Because methane is highly mobile, buoyant and almost insoluble in groundwater, the fault system may act as the conduit, allowing methane to migrate to the soil layer. The carbon dioxide in the soil may originate from the mantle degassing, carbonate dissolution, organic material oxidation and plant breathing (Baubron, *et al.*, 2002). Carbon dioxide is heavier than air and less volatile than most gases, it is accumulated in soil layer forming stable, well defined anomalies. As a decay product of uranium-238, radon (^{222}Rn) is present in relatively high concentrations in uranium-rich rock, such as carboniferous mudstone and coal seam. ^{222}Rn is an inert, radioactive gas with a half-life of 3.82 days. Short half-life of ^{222}Rn restrains its transport in subsurface, so that radon gas generated from a deep origin cannot reach the ground surface unless there exists a preferential flow pathway. Although all shallow soil gas concentration is affected by meteorological

[1] *School of Civil Engineering, The University of Queensland, St Lucia, QLD 4072, Australia, E-mail: y.ma5@uq.edu.au*
[2] *Golder Associates, Toowong, QLD 4066, Australia*

factors (Hinkle, 1994), meteorological variations do not appear to affect anomalous soil gas concentration measurements during sample collecting within a period of a few days, unless there are rainfall events (Margaret, 1991). Rainfall affects soil gas concentration more than any other parameters at all sites. No samples are recommended to be taken for at least two days after a heavy rain because of the downward flushing of soil gas in pore spaces, which decrease soil gas concentrations. However, a small amount of rainfall increase soil gas concentration, as an impermeable barrier is formed at ground surface and soil gas is trapped (Hinkle, 1994). For the site investigation presented here, a depth of 1 m soil gas sampling is chosen in order to reduce the meteorological effects. Furthermore, soil gas survey was conducted over a short period of a relatively dry weather condition.

Another technique used for the investigation is the gamma ray spectrometer. ^{214}Bi is the decay product of ^{222}Rn. The dominant gamma rays from ^{214}Bi are more intense in number and higher in energy than the other ^{222}Rn decay products. As a strong gamma ray emitter, ^{214}Bi is the first radioelement in uranium-238 decay series emitting gamma ray, which could be detected by ground survey (Griffiths, *et al.,* 2010). ^{214}Bi is also a major indicator for the estimation of uranium concentrations in rock/ soil by the gamma ray spectrometry detection method (IAEA, 2003). Because of the positive correlation between radon and ^{214}Bi, it is expected that ^{214}Bi also exhibit relatively higher activities in the soil over the potential fault areas (LaBrecque, *et al.,* 2004). Therefore, a gamma ray spectrometer is applied to measure the ^{214}Bi as a simple and rapid technique.

Subsequently, the field investigation was conducted to combine soil gas mapping and gamma ray survey for the detection and characterization of the fault zones.

STUDY AREA

The field site is located at 24 km North West of Singleton, NSW, Australia (S32.49491°, E150.95169°). The site consists of low undulating slopes and flat lying area with land surface elevations of about 70 m Australian Height Datum (AHD) over most of the floodplain area. A number of monitoring bores provide valuable information of groundwater hydrology. The site is mainly underlain by unconsolidated paleochannel sediments of gravel, silts and clays. The thickness of the alluvial sediments varies from 10 m to 20 m. Soil gas mapping and gamma ray survey were conducted in areas of three different soil types, as shown in Figure 1. The measurement procedure was tested for different soil conditions.

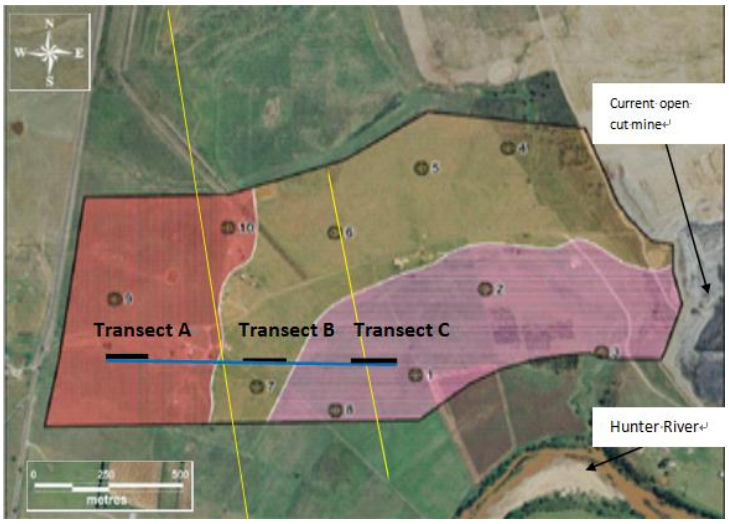

Figure 1 - Satellite image of the top view of the field site

Red area is covered by duplex loam. The brown part is uniform silty clay. The pink area is underlain by uniform silty clay loam (GSS Environmental, 2010). The 10 dots show the soil sampling wells. The two yellow lines are inferred faults crossing the site. The solid black lines are the three transects where soil gas mapping was carried out. Each solid black line is 100 m long with five soil gas measuring points (25 m interval). The blue line is around 1 000 m long, covering all three individual transects. Gamma ray survey was carried out along the blue line with a 10 m interval.

The site is underlain by Permian coal measure strata comprising among others from top down the Vaux, Broonie and Bayswater seams. The interburden comprises sandstone, siltstone and shale (Mackie, 2010). Two inferred fault structures are striking through the site (Figure 1). Those inferred faults increase the likelihood of methane, carbon dioxide and ^{222}Rn migrating through permeable fractures to the ground surface.

Sampling and analysis

In our investigation, conventional active soil gas sampling methods were adopted. The entire sampling procedure is affected by many factors, which could lead to operational errors, such as ambient air intruding the sampling train and soil gas bypassing flow through the annular gap. Three tentative tests were conducted to aim at lessening operational errors prior to mobilizing in the field (Department of Toxic Substance Control, 2010).

Equilibrium time test: Soil gas conditions were disturbed during the probe emplacement. To allow the soil gas to equilibrate to the initial condition, a waiting time between the soil gas probe emplacement and soil gas sampling must be included. This equilibrium waiting time was tested.

Shut-in test (valves, lines, fitting): Prior to purging and sampling, shut-in test were conducted to check the leaks from valves, lines and fittings (above ground portion of sampling train). To evaluate the leaks, a vacuum pump was employed to vacuum the closed tube line. If there is any observable loss of vacuum, the sampling train needs to be redesigned or reconnected.

Purge volume test: The purpose of the purge volume test was to ensure that the ambient and stagnant air was purged out from the sampling system so that samples collected were of representative soil gas conditions.

The active soil gas sampling procedure was divided into three steps:

Soil gas probe emplacement: The probe was placed with the sampling tube into 1 m soil depth (Figure 2). A sealant of hydrated bentonite and air isolation packer were applied to seal off the annular gap around the probe. The hydrated bentonite was prepared by mixing one portion of powder bentonite with four portions of water, giving a gel-like end product.

Soil gas sampling procedure: 28 ml soil gas samples were taken by syringe. Soil gas samples were injected into the vacuum Labco exetainer. The volume of the vacuum exetainer is 12 ml. The more volume of gas is injected, the higher exetainer inner pressure is gained. If a leakage occurred, the gas would leak from inside to outside instead of air coming into the exetainer. This procedure prevents ambient air from entering the vacuum exetainer to dilute the soil gas sample. To check the reproducibility, replicate samples were taken for each point. The samples stored in the glass exetainers were analysed off-site in the lab by gas chromatography.

Helium tracer gas application: The most common errors of soil gas sampling are due to leakages along the sampling tube where the tube is in contact with the soil (ring gap) (Department of Toxic Substance Control, 2010). A tracer gas method was developed to check the effectiveness of the sealant, which was applied to avoid the breakthrough of air down to the probe, as shown in Figure 2.

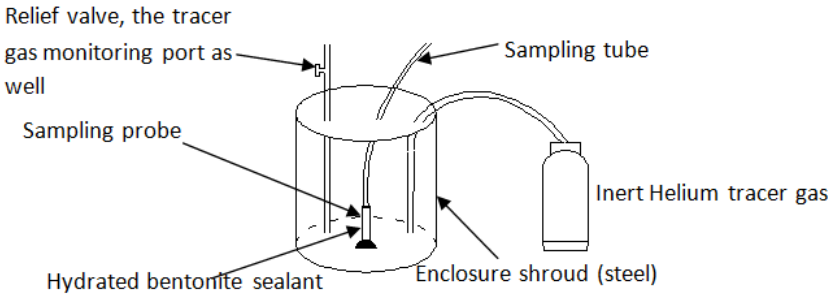

Figure 2 - Schematic of the tracer gas method

The shroud was manufactured with three screw fixing rubbers on top, which were expected to stop bypassing leakage at the connecting points. The volume of the shroud was around 11.5 L. The helium gas cylinder (GOREGAS) was filled by 99.9% helium.

Helium tracer gas testing was conducted in the following steps:

1) Place the enclosure shroud over the probe on the ground;
2) Pull the sampling tube out of the shroud;
3) Seal the bottom shroud with hydrated bentonite;
4) Connect helium gas cylinder to the shroud, and open the relief valve;
5) Slowly inject the tracer gas into the shroud, and monitoring the helium concentration at the port of the relief valve with hand-held helium detector (GasCheck G3);
6) When the helium concentration approximately reach 0.2%, stop the tracer gas injection, and close the relief valve;
7) Take the 28 ml soil gas sample with syringe;
8) Helium concentration is measured by the pin detector at the tail-end of the sampling tube.

Finally, the dilution factor is calculated with the soil gas helium concentration divided by the shroud helium concentration. If the dilution factor is less than 5%, the samples are relatively acceptable (Department of Toxic Substance Control, 2010). Otherwise, the soil gas needs to be re-sampled.

Radon measurements

Measurements of ^{222}Rn concentrations in the soil gases were carried out using the RAD7 portable radon detector (Durridge, USA). It contains a solid-state silicon alpha detector and a built-in pump with a flow rate of around 1 l/min. The inlet filter blocks fine dust particles and radon daughters entering the RAD7 testing chamber. The soil gas measurements are carried out in the sniff mode, which calculates ^{222}Rn concentrations from the data in window A only. The sniff mode covers the energy range from 5.40 to 6.40 MeV, showing the total counts from 6.00 MeV alpha particles of the ^{218}Po decay (daughter of ^{222}Rn).

^{214}Bi measurement

The ^{214}Bi measurements were made by the uranium channel of the GR-320 differential gamma ray spectrometer (Terraplus, Canada). The channels and energy ranges are shown in Table 1. The 0.35l NaI detector was placed vertical on the soil surface with a counting period of 100 seconds. Vegetation and small stones were removed before the measurement. The spectra were recorded and the Noise-Adjusted Singular Value Decomposition (NASVD) method was applied to process the spectrum.

Table 1 - Measuring nuclide, energy and channel range for the K, U and Th in the gamma ray spectrometer analysis

Window of interest			
	Potassium	Uranium	Thorium
Nuclide	^{40}K (1.460MeV)	^{214}Bi (1.765MeV)	^{208}Ti (2.614MeV)
Channel range	111-126	133-149	192-223
Energy(MeV) range	1.365-1.557	1.647-1.854	2.420-2838

Results and discussions

Results of soil gas mapping and gamma ray survey

Soil gas concentrations are shown in Table 2. The range of CH_4 concentration is relatively low, maybe because of the coal seam methane degassing in/ from the adjacent open-cut pit. The average dilution factor of radon is higher than those of the CO_2 and CH_4, due to more soil gas pumping in the course of radon measurement.

Table 2 - Three transects' soil gas concentrations for CO_2, CH_4 and Rn. DF1 is the dilution factor for CO_2 and CH_4, DF2 shows the dilution factor of Rn. All presented data have been corrected based on the dilution factor.

Location	CO_2 (%)	CH_4 (ppm)	DF1	Rn (kBq/m3)	DF2
A1	0.18	1.43	2.70%	0.04	15%
A2	0.14	2.38	3.60%	3.86	31%
A3	0.95	0.68	0.24%	20.58	2.70%
A4	0.61	2.72	0.71%	0.09	16.60%
A5	1.58	0.20	0.78%	18.77	0.75%
B1	1.65	0.19	9.41%	28.14	1.48%
B2	1.17	0.42	0.76%	26.83	5.90%
B3	1.35	0.26	1.70%	36.76	4.30%
B4	1.57	0.25	1.40%	21.40	1.74%
B5	1.72	0.20	0.65%	27.13	0.40%
C1	1.64	0.24	1.00%	28.64	1.90%
C2	2.35	0.26	0.59%	22.71	0.80%
C3	2.00	0.22	0.45%	21.16	1%
C4	1.90	0.23	1.59%	21.69	1.55%
C5	1.86	0.20	0.50%	17.13	0.30%

To examine the corresponding correlation between different parameters, the normalized gamma ray, radon, CO_2 and CH_4 are plotted in Figure 3. ^{214}Bi signals in the U window are chosen to represent the gamma ray data. In this application, the statistical threshold for gamma ray anomalous values was fixed at "mean value+1/2 standard deviation". Above this threshold, no change is applied to raw data, below this threshold, the raw data is set to zero.

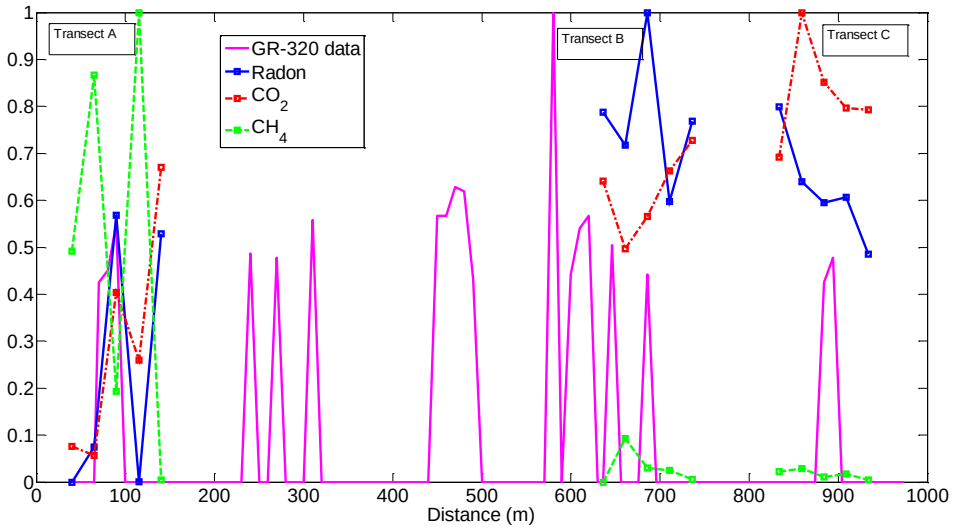

Figure 3 - Radon, CO_2, CH_4 and GR-320 measurement values are normalized. Gamma ray data from the U window represents ^{214}Bi signals. The squares show the measuring points.

In Figure 3, higher CH_4 concentrations are evident in transect A. However, lower radon and CO_2 concentrations are also shown. In transect B, the radon value is relatively high, and the CO_2 concentration is lower compared with transect C. The maximum CO_2 concentration appears in the transect C. No clear corresponding correlation between the gamma ray, CO_2, CH_4 and radon concentrations can be identified from the results shown in Figure 3. This may reflect the complexity of signals of soil gas and gamma ray at the site. On the other hand, as soil gas follow the permeable

pathway formed by faults and fracture zones, the measurement of higher soil gas concentration may illustrate the existence of permeable structure, but the relatively small database could not show any anomaly from the soil gas concentration.

Grasty (1987) showed that 98% gamma ray radiation comes from the top 35 cm of the earth crust. However, in this layer the radon concentration is highly variable because of variable barometric pressure, water content and gas permeability. Field experiments show different correlations between ^{214}Bi concentration and radon concentration in different environments. Vulkan and Shirav (1997) found good correlation between ^{214}Bi measured by an airborne gamma ray spectrometer and ^{222}Rn concentration in an arid area, where a soil layer was almost absent. However in the semi-arid and humid areas, the correlation is poor.

Carbon dioxide and light hydrocarbon (such as methane) could easily migrate through more permeable structures. It contributes to higher concentrations of the light hydrocarbon and carbon dioxide in the upper soil layer. Because of this light hydrocarbon accumulation, Price (1986) concluded that hydrocarbon-consuming bacteria (hydrocarbon oxidizing activity) would significantly influence the near surface geochemical environment. As a result, light hydrocarbons are oxidized to carbon dioxide and lead to acidic condition in the soil and pore water. This microbial activity may be another reason for the lower methane background. The acidic environment created by the hydrocarbon degradation could also build up the uranium concentration in the soil layer, which leads to increased gamma ray emission.

NASVD method

To improve the data interpretation, the noise in the gamma ray data should be filtered. The main factors that reduce the assay precision are the statistical nature of radiation, variable background and variable water content in the soil. High soil moisture could block the radiation flux. 10% increase in soil moisture will decrease about the same amount of radiation flux from the soil surface (Minty, 1997). The statistic of radioactive decay in a particular time interval follows the Poisson statistical distribution (Frigerio, 1974). The gamma ray background is originated from the atmospheric radon, cosmic background and fallout materials from nuclear accidents, such as Chernobyl nuclear accident. It does not reflect the geological information and needs to be removed from the observed gamma ray spectra.

A statistical approach was proposed by Hovgaard (1997) to extract signals in the multichannel raw spectra, called Noise-Adjusted Singular Value Decomposition (NASVD). NASVD is a procedure for removing noise from the raw gamma ray spectra using the spectral component analysis method. The observed spectra are scaled to the unit variance in each channel. Then, eigenvectors are calculated and rescaled by multiplying the unit average spectrum. The lower-order components represent signal in the original observed spectra, and the higher-order components represent noise. The noise is removed by reconstructing the spectra from the lower order eigenvectors and amplitudes (Minty and McFadden, 1998). The "cleaned" spectra are then processed using a standard 3-windows method to extract K, U and Th window data.

The first 16 eigenvectors from the NASVD analysis of raw spectra are shown in Figure 4. The coherent spectral shape is shown in the lower order eigenvector, and these are interpreted to represent the signal in the input spectra. The higher-order eigenvectors do not show evidence of coherent spectral shape, and these are mainly noise.

The comparison of the NASVD processed spectra with the raw spectra is shown in Figure 5. In the U window, the processed spectra showed a peak point and a clearer trend, compared with the more oscillatory raw spectra.

The precision of the field assays is expected to be about 0.1% K, 0.4 ppm eU and 0.6 ppm eTh (IAEA, 2003). However, at our field site the mean values were 0.1% K, 0.25 ppm eU and 0.41 ppm eTh. The media values were 0.1% K, 0.2 ppm eU and 0.4 ppm eTh. All these values are around the detection limit of the field survey, which means the background value is very low. The sensitivity level of the detector for the U window is 0.325 counts per second, and nearly all the U window counts were around this sensitivity level. In Figure 6(a), the NASVD processed data in U window do not reflect any trend compared with original spectra result in U window. In Figure 6(b), the error bars are plotted in each measurement point. It can be seen that almost all signals are strongly affected by the noise. The dot black line showing the benchmark passes through the majority of error bars with all the gamma ray data within the noise variation range, indicating that nearly no significant ^{214}Bi signals were detected.

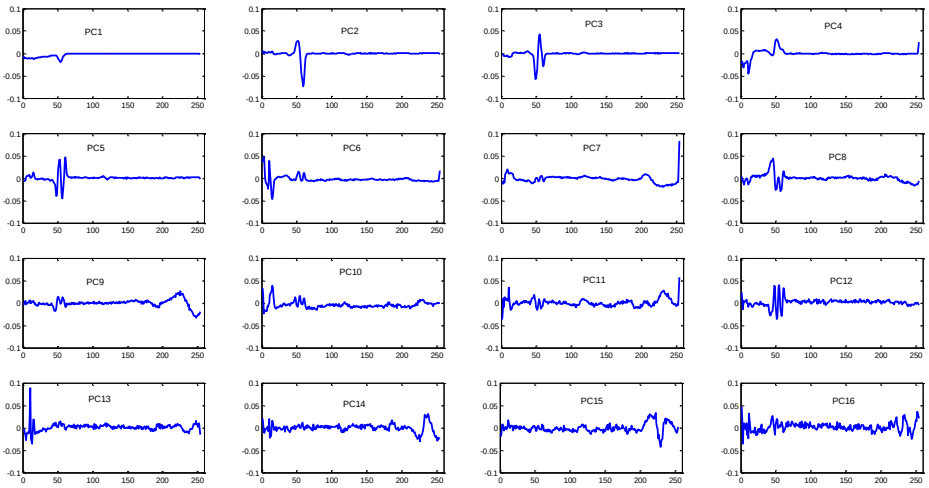

Figure 4 - NASVD eigenvectors from field test spectra. PC is the principle component

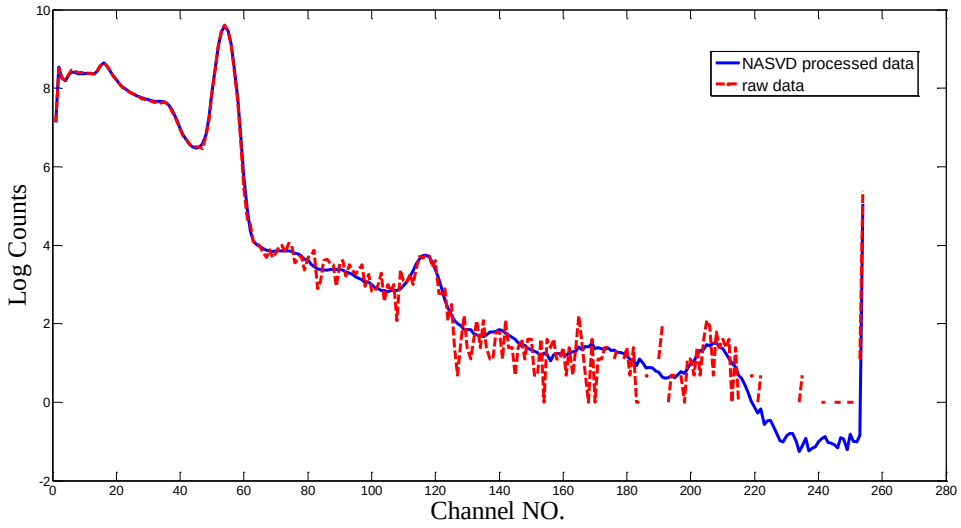

Figure 5 - The comparison of NASVD processed spectra with original spectra

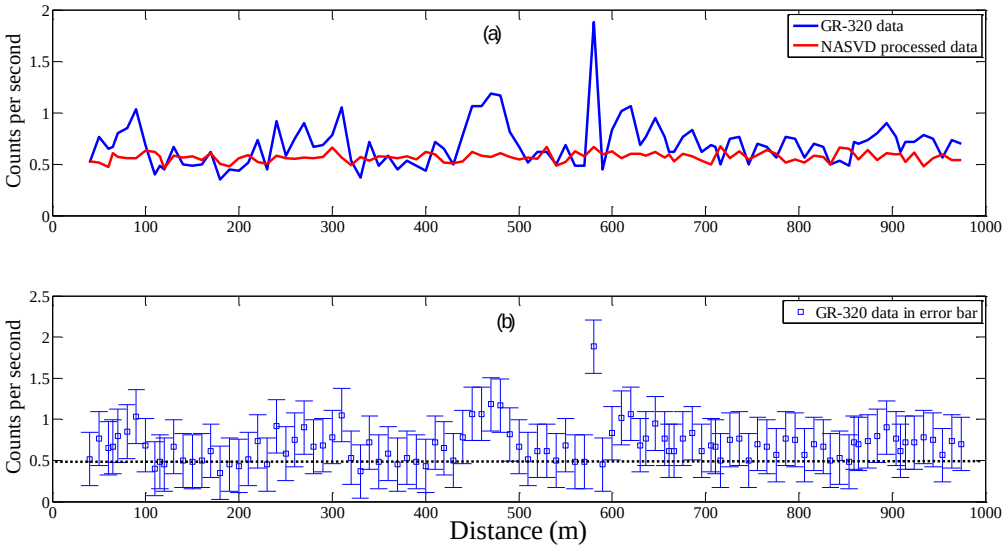

Figure 6 - (a) Gamma ray survey result of the U window along the whole transect with the comparison of the NASVD processed data; (b) Gamma ray result of the U window with error bars, and the dot black line shows the benchmark

CONCLUSIONS

The field experiment has demonstrated the complexity of the soil gas migration and gamma ray emission.

The limitation of the soil gas mapping method lies in the weak crustal gas concentration in case of the thick sedimentary cover, such as alluvial soil layer (average 20 m alluvial soil layer cover the rock and coal seam at this site), leading to the spread of gases through the soil layer which broadens the anomalies. Environmental influence in the near surface soil layer may also contribute to weakening the signals. Only careful design of soil gas sampling programmes can increase the probability of detecting faults by soil gas mapping. Regarding the gamma ray survey, the gamma ray background signal seems too weak for detection. Further study is required to understand this complex system, in particular,

- How to differentiate the geogenic and biogenic sources for methane, carbon dioxide?
- How to distinguish the radon origin of deep host rock from that due to uranium mineral in the upper soil layer?

ACKNOWLEDGEMENTS

The research project has been funded by the Australia Coal Association Research Program (ACARP C20022). The authors are also grateful for the support of RTCA Hunter Valley Operations.

REFERENCES

Baubron, J C, Rigo, A and Toutain, J P, 2002. Soil gas profiles as a tool to characterise active tectonic areas: the Jaut Pass example (Pyrenees, France), *Earth and Planetary Science Letters,* 196, pp 69-81.

Department of Toxic Substance Control, 2010. *Advisory - Active soil gas investigation*, Cypress, CA.

Frigerio, N A, 1974. Poisson and non-poisson behavior of radioactive systems, *Nuclear Instruments and Methods,* 114, pp 175-177.

Grasty, R L, 1987. Design, construction and application of airborn gamma-ray spectrometer calibration pads-Thailand, Geological Survey of Canada, pp 87-88 (Ottawa, Canada).

Griffiths, A D, Zahorowski, W, Element, A and Werczynski, S, 2010. A map of radon flux at the Australian land surface, *Atmospheric Chemistry and Physics,* 10, pp 8969-8982.

GSS. Eenvironmental, 2010. Soil Survey and Land Resource Assessment Carrington West Wing, pp 8-11.

Hinkle, M E, 1994. Environmental conditions affecting concentrations of He, CO2, O2 and N2 in soil gases, *Applied Geochemistry,* 9, pp 53-63.

Hovgaard, J, 1997. A new processing technique for airborne gamma-ray spectrometer data (Noise Adjusted Singular Value Decomposition), in *proceedings Am. Nucl. Soc. Sixth topical meeting on Emergency Preparedness and Response 1997*, pp 123-127, (San Fransisco).

IAEA, 2003. Guidelines for radioelement mapping using gamma ray spectrometry data, International Atomic Energy Agency, pp 39-40 (Vineea).

Labrecque, J, Melo, L, Cordoves, P and Urbani, F, 2004. A simple and rapid method to locate fault traces by measurements of 214 Bi in soils, *Journal of Radioanalytical and Nuclear Chemistry,* 261, pp 343-347.

López, D L and Smith, L, 1995. Fluid flow in fault zones: Analysis of the interplay of convective circulation and topographically driven groundwater flow, *Water Resources Research,* 3, pp 1489-1503.

Mackie, C D, 2010. *Coal and Allied Carrington West Wing Modification Groundwater Assessment*, March 2010.

Margaret, E H, 1991. Seasonal and geothermal production variations in concentrations of He and CO2 in soil gases, Roosevelt Hot Springs Known Geothermal Resource Area, Utah, U.S.A. *Applied Geochemistry,* 6, pp 35-47.

Minty, B and Mcfadden, P, 1998. Improved NASVD smoothing of airborne gamma-ray spectra, *Exploration Geophysics,* 29, pp 516-523.

Minty, B R S, 1997. Fundamentals of airborne gamma-ray spectrometry, *AGSO Journal of Australian Geology and Geophysics,* 17, pp 39-50.

Price, L C, 1986. A critical review and proposed working model of surface geochemical exploration, MJ Davidson, ed., *Unconventional methods in exploration for petroleum and natural gas IV*. Dallas, Southern Methodist University Press, pp 245-304.

The NSW Office of Water, 2011. The NSW Aquifer Interference Policy - protecting our groundwater systems, In *Industries*, D. O. P. (Ed.).

Vulkan, U and Shirav, M, 1997. Radiometric Maps of Israel-Partial Contribution to the Understanding of Potential Radon Emanations, in *Proceedings Uranium Exploration Data and Techniques Applied to the Preparation of Radioelement Maps 1997*, pp 119-124 (Vineea).